Time-dependent density-functional theory simulation for electron–ion dynamics in molecules under intense laser pulses

2009 J. Phys.: Condens. Matter 21 064222

(http://iopscience.iop.org/0953-8984/21/6/064222)

J. Phys.: Condens. Matter **21** (2009) 064222 (5pp) doi:10.1088/0953-8984/21/6/064222

Time-dependent density-functional theory simulation for electron–ion dynamics in molecules under intense laser pulses

Y Kawashita[1], **T Nakatsukasa**[2,3] **and K Yabana**[1,2,3]

[1] Graduate School of Pure and Applied Sciences, University of Tsukuba, Tsukuba 305-8571, Japan
[2] Center for Computational Sciences, University of Tsukuba, Tsukuba 305-8577, Japan
[3] Theoretical Nuclear Physics Laboratory, RIKEN Nishina Center, Wako 351-0198, Japan

E-mail: kawashita@nucl.ph.tsukuba.ac.jp

Received 29 June 2008, in final form 17 November 2008
Published 20 January 2009
Online at stacks.iop.org/JPhysCM/21/064222

Abstract
We have developed a simulation method to describe three-dimensional dynamics of electrons and ions in a molecule based on the time-dependent density-functional theory. We solve the time-dependent Kohn–Sham equation for electrons employing the real-space and real-time method, while the ion dynamics are described in classical mechanics by the Ehrenfest method. For an efficient calculation in massively parallel computers, the code is parallelized dividing the spatial grid points. We apply the method to the Coulomb explosion of the H_2S molecule under an intense and ultrashort laser pulse and investigate the mechanism of the process.

1. Introduction

The time-dependent density-functional theory (TDDFT) [1] has been rapidly developing as a tool to describe electronic excitations and dynamics in atoms, molecules and solids. The applications of the TDDFT are classified into two categories. One is the linear response regime in which the external field is treated as a perturbation [2–4]. The electronic excitations and linear optical responses have been described quite successfully in this approach. The other is the application to nonlinear and nonperturbative dynamics of electrons induced, for example, by the intense laser field [5–9].

We have developed a computational method to solve the time-dependent Kohn–Sham (TDKS) equation in real-time which can be applied to both linear response and nonlinear dynamics [2, 10–12], in which a uniform grid representation in the three-dimensional Cartesian coordinate is employed. Recently we have implemented an efficient parallelization in our code, dividing the spatial area by xy, yz and zx planes. This parallelization scheme works efficiently as reported in the literature [13–15]. The parallel computation has enabled us to calculate phenomena which require a calculation in a wide spatial area. In the present paper, we report an application of our method to the Coulomb explosion of molecules induced by an intense and ultrashort laser pulse.

It has been well known that atoms and molecules under intense and ultrashort laser pulses exhibit various interesting phenomena reflecting nonlinear and nonperturbative electron dynamics [16–18]. Under irradiation by the intense laser pulse, a molecule loses multiple electrons, instantaneously forming the highly charged molecule. The ionization occurs either by multiphoton or tunneling ionization mechanisms [19]. The highly charged molecule then explodes by Coulomb repulsion between ions [18]. Experimentally, the Coulomb explosion imaging technique has been developed and has enabled us to observe the ionic motion of molecules on a timescale of a few femtoseconds after the explosion. This technique was first applied to diatomic molecules and then to polyatomic molecules [20–22]. We will calculate the Coulomb explosion dynamics taking the H_2S molecule as an example [23]. The calculated results will be compared with measurements to obtain a microscopic understanding of the mechanisms.

The organization of this paper is as follows. In section 2, we give a brief explanation of the real-time calculation of the TDKS equation. In section 3, we discuss the choice of the exchange–correlation potential to be used in our calculation. We then explain our parallel computation in section 4. In section 5, we show our analyses for the Coulomb explosion of the H_2S molecule for which a measurement has been reported recently. A summary will be presented in section 6.

2. TDDFT description for electron–ion dynamics

We describe the electron dynamics solving the TDKS equation for the orbital wavefunctions, $\psi_i(\vec{r}, t)$:

$$i\hbar\frac{\partial}{\partial t}\psi_i(\vec{r}, t) = \left\{-\frac{\hbar}{2m}\nabla^2 + V_{\rm ion}(\{\vec{R}_a\}) + e^2\int d\vec{r}'\frac{\rho(\vec{r}', t)}{|\vec{r} - \vec{r}'|} + V_{\rm xc}[\rho(\vec{r}, t)] + V_{\rm ext}(\vec{r}, t) - iW(\vec{r})\right\}\psi_i(\vec{r}, t), \quad (1)$$

where $\rho(\vec{r}, t)$ is the electron density given by $\rho(\vec{r}, t) = 2\sum_i |\psi_i(\vec{r}, t)|^2$, $\vec{R}_a$ is the coordinate of the ath ion and $V_{\rm ext}(\vec{r}, t)$ is the potential of the applied laser pulse, $V_{\rm ext}(\vec{r}, t) = e\vec{E}(t)\cdot\vec{r}$. We assume the following form for the electric field of the laser pulse:

$$E(t) = \begin{cases} E_0 \sin^2\dfrac{\pi t}{T}\sin\omega t & \text{for } 0 \leqslant t \leqslant T \\ 0 & \text{for } T < t \end{cases} \quad (2)$$

where T and ω are the length and the frequency of the laser pulse, respectively. $V_{\rm ion}(\{\vec{R}_a\})$ is the electron–ion potential for which we employ the Troullier–Martin norm-conserving pseudopotential with a separable approximation [24, 25]. $V_{\rm xc}[\rho(\vec{r}, t)]$ is the exchange–correlation potential. We employ the simple adiabatic local-density approximation (ALDA) in our calculation. In section 3, we explain the reason of this choice. $-iW(\vec{r})$ is the absorbing potential which is placed far outside the molecule. This potential removes the unfavorable reflection of electrons at the boundary.

To calculate the time evolution of the wavefunction, we assume that, for a short period $t \to t + \Delta t$, the time evolution of the wavefunction may be described with the Kohn–Sham Hamiltonian at a time t:

$$\psi_i(\vec{r}, t + \Delta t) \simeq e^{-i(h_{\rm KS}[\rho(\vec{r},t),\{\vec{R}_a\}])\Delta t/\hbar}\psi_i(\vec{r}, t). \quad (3)$$

We then employ a Taylor expansion method to achieve the time evolution:

$$\psi_i(\vec{r}, t + \Delta t) \simeq \sum_{k=0}^{k_{\rm max}}\frac{1}{k!}(-i(h_{\rm KS}[\rho(\vec{r}, t), \{\vec{R}_a\}])\Delta t/\hbar)^k\psi_i(\vec{r}, t), \quad (4)$$

where we take $k_{\rm max} = 4$ [2].

In describing the orbital wavefunctions, we employ a uniform spatial grid representation in the three-dimensional Cartesian coordinate. A high-order finite difference method with nine-point formula is used for the Laplacian operation [27]. In all the calculations below, we use a spatial mesh spacing of 0.211 Å and a time step of $\Delta t = 0.968$ as.

We describe the ion dynamics by Newton's equation of motion where the forces acting on ions are evaluated from the electron-density distribution at each time step:

$$M_a\frac{d^2}{dt^2}\vec{R}_a = \vec{F}_a^{\rm elec-ion} + \vec{F}_a^{\rm ion-ion} + \vec{F}_a^{\rm ext-ion}, \quad (5)$$

$$\vec{F}_a^{\rm elec-ion} = -\int d\vec{r}\frac{\partial V_{\rm ion}(\vec{r}, \vec{R}_a)}{\partial\vec{R}_a}\rho(\vec{r}, t), \quad (6)$$

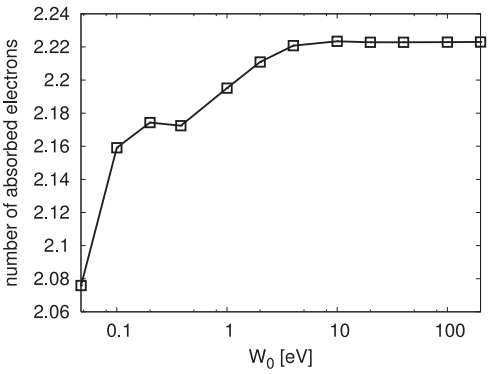

Figure 1. The number of absorbed electrons as a function of the strength of the absorbing potential, W_0, when the H_2S molecule is irradiated by the laser pulse. See the text for details.

$$\vec{F}_a^{\rm ion-ion} = e^2\sum_b\frac{Z_aZ_b(\vec{R}_a - \vec{R}_b)}{|\vec{R}_b - \vec{R}_a|^3}, \quad (7)$$

$$\vec{F}_a^{\rm ext-ion} = eZ_a\vec{E}(t), \quad (8)$$

where eZ_a is the electric charge of ion a. The time propagation of ions is achieved by using the Verlet algorithm as follows:

$$\vec{R}_a(t + \Delta t) = 2\vec{R}_a(t) - \vec{R}_a(t - \Delta t) + \frac{\vec{F}_a(t)}{M_a}\Delta t^2, \quad (9)$$

where $\vec{F}_a$ is the force acting on the ion, the sum of the three forces given in equations (6)–(8). We solve the coupled equations for electrons, equation (1), and for ions, equation (5). Before laser irradiation, the ions are located at their equilibrium positions and the electron orbitals are the ground state solutions of the Kohn–Sham equation.

For the absorbing potential, we take a linear dependence of the radial variable, $-iW(\vec{r}) = -iW_0(r - R)/\Delta R$ for $R < r$ and $-iW(\vec{r}) = 0$ for $0 < r < R$. We choose R and ΔR as $R = 8.46$ Å and $\Delta R = 4.23$ Å. The value of W_0 should be so chosen that the number of absorbed electrons is not sensitive to the parameters. In figure 1, we show the number of absorbed electrons changing the value of W_0 when an H_2S molecule is irradiated by the laser pulse of frequency $\hbar\omega = 1.55$ eV, pulse length $T = 24$ fs and laser intensity 1×10^{15} W cm^{-2}. It is clearly seen that the number of absorbed electrons is not sensitive to the value of W_0 for $W_0 > 5$ eV. In the following calculations, we take $W_0 = 13.6$ eV.

3. Choice of the exchange–correlation potential

Although a simple ALDA for the exchange–correlation potential has been known to provide a reasonable description for electronic excitations of many molecules, it has been clarified that the ALDA fails on several occasions. In atoms and molecules under an intense laser pulse, it has been clarified that the ALDA overestimates the ionization rate of the neutral atoms and molecules substantially [19]. This failure is related to the underestimation of the orbital energy in the LDA. To obtain the correct ionization rate, it is important to employ the exchange–correlation potential which

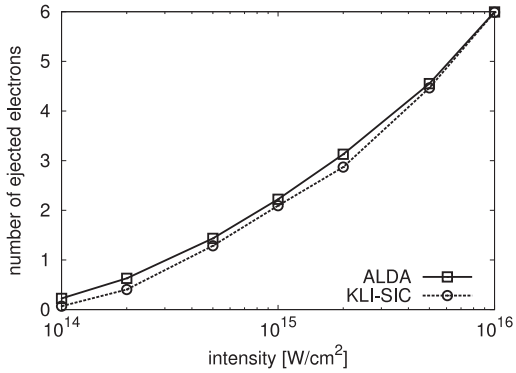

Figure 2. The number of ejected electrons from the H_2S molecule as a function of the intensity of the irradiating laser pulse. The pulse length and frequency are $T = 24$ fs and $\hbar\omega = 1.55$ eV, respectively.

takes account of the self-interaction correction (SIC). As an approximate procedure with SIC, the KLI-SIC method [26] has often been employed [7, 19]. In figure 2, we show the number of removed electrons from the H_2S molecule under a laser pulse of various intensities. The results with the ALDA and with the KLI-SIC are compared. As is seen in the figure, the ionization rate in the ALDA is much larger than that in the KLI-SIC when the laser intensity is weak ($\sim 10^{14}$ W cm^{-2}), while there is only a very small difference when many electrons are removed. This result suggests that the problem of the LDA is not significant when many electrons are ionized. We also note that, since the expression for the total energy functional is not known in the KLI-SIC approach, it is not possible to calculate the forces acting on ions. Another well-known failure of the ALDA in laser–atom interaction is the difficulty in describing the nonsequential double ionization in atoms, which is caused by the rescattering process [28]. At present, no simple prescription is available for the exchange–correlation potential to describe it [29, 30]. Under these circumstances, we consider that it should be a reasonable choice to employ the ALDA to describe the Coulomb explosion phenomena. We note that the ALDA has often been employed in laser–atom and laser–molecule interactions in the literature [8, 31, 9, 32, 33]. We also note that the limitation of the KLI-SIC method had been pointed out recently, see [34]. In [35], a new scheme for the TD-SIC method is proposed.

4. Parallelization of the computational code

The uniform grid representation in the three-dimensional Cartesian coordinate, which we adopt for the description of electron orbitals, is suited for efficient parallel computation by dividing the spatial grid points. We have implemented a parallelization in our computational code written in Fortran90 with the message-passing interface. In our algorithm, the time evolution of the orbital wavefunctions is achieved by successive operations of the Kohn–Sham Hamiltonian on the orbital wavefunctions. We also need to solve the Poisson equation to obtain the Hartree potential at each time step. The operation of the Laplacian is included in both calculations. Since the operation is repeated at each time step and there are so many time steps, typically 50 000, the most time-consuming part in our calculation is the operation of the Laplacian in calculating the time evolution of the wavefunction and in solving the Poisson equation.

Table 1. Comparison of the total elapsed and the communication time for two cases with 64 and 256 processors. In both cases, each processor deals with 30^3 grid points.

	Total elapsed (s)	Communication (s)
256 CPU	1095	345
64 CPU	913	263

The parallelization by dividing the spatial grid points shows a good balance between the computational and the communication costs. Suppose we divide grid points into cubic regions containing M^3 grid points. The calculation of the Laplacian requires $(6N_d + 1)M^3$ operations, where N_d is the number of grid points in one direction required in the high-order finite-difference formula. Before the operation of the Laplacian, exchange of data of $N_d M^2$ grid points are necessary between the six neighboring processors. Since these numbers are independent of the total number of processors, the parallelization by dividing the spatial grids will be quite suitable for the calculations in massively parallel computers.

In table 1, we show the total elapsed and the communication time for a test calculation with 64 and 256 processors achieved at PACS-CS, University of Tsukuba. In this test calculation, each processor deals with 30^3 grid points, the number of time steps is 2500 and the number of Kohn–Sham orbitals is 5 (N_2 molecule). It is clearly seen that the total elapsed time is almost the same for the two cases, although the spatial grid points are four times different. In this test case, the communication time is about 30% of the total elapsed time.

5. Application to Coulomb explosion of H_2S molecule

As an application of our approach, we study the Coulomb explosion of the H_2S molecule under an intense and ultrashort laser pulse. When a molecule is irradiated by a laser pulse whose intensity exceeds 10^{15} W cm^{-2}, multiple electrons are removed instantaneously from the molecule. The highly charged molecule will then explode by the Coulomb repulsion between ions. Experimentally, the momenta and the kinetic energies of the fragments are detected. These observables provide information on the ultrafast dynamics of electrons and ions, shorter than a few tens of femtoseconds, during the Coulomb explosion process.

Recently, a Coulomb explosion experiment has been achieved for a three-atom molecule, H_2S [23]. After forming H_2S^{3+}, the molecule breaks up into three fragments, $S^+ + H^+ + H^+$. The measurement has revealed an interesting fact that there is a strong correlation between the momenta of final fragment ions and the direction of the laser polarization. This is interpreted as reflecting that the Coulomb explosion mechanism depends on the relative orientation between the molecular axis and the laser polarization. We have achieved three calculations, changing the relative orientation between the laser polarization and the molecular axes. The molecular

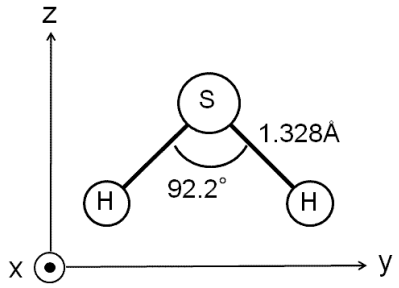

Figure 3. Geometry and molecular axes of the H_2S molecule in the ground state.

axes and geometry are shown in figure 3. The numerical calculation is achieved employing 120^3 grid points.

In the calculations shown below, we will employ a laser pulse of pulse length $T = 24$ fs, intensity $I_n = 1 \times 10^{15}$ W cm^{-2} and frequency $\hbar\omega = 1.55$ eV. The pulse length and laser frequency are close to those of the experiment. However, the laser intensity employed in the experiment is 2×10^{14} W cm^{-2}, five times smaller than that employed in our calculation. We first discuss the number of emitted electrons, which is equal to the sum of the charge number of the final fragmented ions. In the TDDFT calculation, the final charge of each fragment ion is uniquely determined for a given laser pulse, and is fractional. On the other hand, the measured final charge states are, of course, always integer. The fragment ions also show a distribution in several charge states for a given laser pulse. The intensity of the laser pulse employed in our calculation, 1×10^{15} W cm^{-2}, is so chosen that the molecule loses approximately three electrons by laser irradiation. To compare the measurements with the TDDFT calculation, it would be reasonable to compare the average charge number of the measured fragments in different charge states with the calculated results.

For three directions of polarization parallel to $\hat{x}$, $\hat{y}$ and $\hat{z}$, the number of emitted electrons is calculated to be 2.5, 3.5 and 2.6, respectively. This result indicates that the molecule is most easily ionized when the laser polarization is parallel to the direction connecting two hydrogen atoms ($\hat{y}$ direction). Experimentally, the momenta of the final fragments of S^+, H^+ and H^+ are measured. It has been reported that a high yield is observed when the relative momentum of two hydrogen ions H^+ aligns in the direction of the laser polarization [23].

Table 2. The momentum angle θ_{12} and the KER are shown for three cases of laser polarization. The KER normalized to the three-charge state is shown as well. See the text for details.

	θ_{12} (deg)	KER (eV)	KER (normalized) (eV)
$\hat{x} \parallel \epsilon$	164	8.36	12.04
$\hat{y} \parallel \epsilon$	118	25.8	18.96
$\hat{z} \parallel \epsilon$	152	12.0	15.98

Thus our calculation shows a good correspondence with the measured trend.

We next consider the angle between the momenta of two hydrogen ions H^+ after the Coulomb explosion which we denote as θ_{12}, and the kinetic energy release (KER), which is the sum of the kinetic energies of the three final fragment ions, $E_{\mathrm{KER}} = \sum_i \vec{p}_i^{\,2}/(2m_i)$, where p_i and m_i are the momentum and mass of each fragment (S^+, H^+, H^+).

Figure 4 shows the behavior of θ_{12} as a function of time. Initially, in the ground state, the angle between two S–H bonds is 92.8°. If we assume that the electron emission occurs instantaneously and the Coulomb explosion takes place after the ionization is ended, the angle between two H^+ ions, θ_{12}, should be close to the bond angle. However, the calculation shows that the final angle between hydrogen fragments is always larger than the initial bond angle for three cases of polarization.

In table 2, we show the KER as well as the final angle θ_{12} in three cases of laser polarization. Since the final charge state is not the same in three cases, we also show the KER normalized to the three-charge state. Namely, for a calculated charge state of q, the KER is multiplied by $(3/q)^2$. If we calculate the static Coulomb potential of three point charges e at the equilibrium positions of S and H ions in the ground state of H_2S, the potential energy is 29.2 eV. This is considered the upper limit of the KER when the ionization occurs instantaneously. The calculated KER is always lower than this value for three cases of polarization. We also find the correlation that the lower the kinetic energy release is the larger the angle θ_{12} is.

Now we compare the calculated results with the measurements [23]. In the measurements, the angle between hydrogen ions is reported to be larger than the initial bond angle, consistent with the calculation. In the measurements, the KER is larger as the angle θ_{12} is smaller, again consistent with

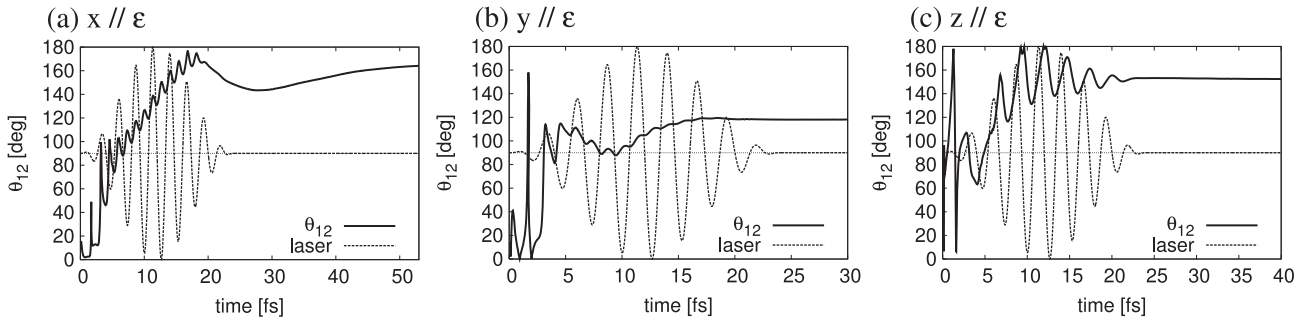

Figure 4. The angle θ_{12} as a function of time is shown for the cases of (a) laser polarization direction parallel to the $\hat{x}$ direction, (b) parallel to the $\hat{y}$ direction and (c) parallel to the $\hat{z}$ direction.

the calculation. However, in the measurements, the correlation between the angle θ_{12} and the direction of laser polarization is opposite to the present calculation. In the measurement, when the difference of the two momenta of the H^+ ion is parallel to the laser polarization, which corresponds to the case of $\hat{y}$ polarization, the angle θ_{12} is the largest, contrary to our calculation.

At present, we do not have any explanation for this discrepancy. One possible origin of the discrepancy may be a rotation of the molecule during laser irradiation. We calculated only the cases where the laser polarization direction coincides with one of the axes of inertia, and have found no rotational motion of the molecule in our calculation. However, when the direction of the laser polarization does not coincide with the axes of inertia, the molecule may rotate during the laser irradiation, which will affect the final direction of the fragmented ions.

6. Summary

We have discussed the implementation and the application of the TDDFT with Ehrenfest ion dynamics to simulate the three-dimensional electron–ion dynamics. The time-dependent Kohn–Sham equation is solved with the real-space and real-time method and the code is parallelized by dividing the spatial region. We applied the method to the Coulomb explosion of the H_2S molecule. It is shown that the calculations reproduce several features of the measurement including the dependence of the ionization rate on the direction of laser polarization and increase of the bond angle during the Coulomb explosion. However, a discrepancy remains in the correlation between the direction of the fragment momenta and laser polarization.

Acknowledgments

The numerical calculations are achieved by the massively parallel cluster PACS-CS, University of Tsukuba, and the supercomputer at the Institute of Solid State Physics, University of Tokyo. This work is supported by the Grant-in-Aid for Scientific Research (nos. 19019002, 18540366 and 17540231).

References

[1] Runge E and Gross E 1984 *Phys. Rev. Lett.* **52** 997
[2] Yabana K and Bertsch G F 1996 *Phys. Rev.* B **54** 4484
[3] Jamorski C, Casida M E and Salahub D R 1996 *J. Chem. Phys.* **104** 5134
[4] Nakatsukasa T and Yabana K 2001 *J. Chem. Phys.* **114** 2550
[5] Gross E K U, Dobson J F and Petersilka M 1996 *Top. Curr. Chem.* **181** 81
[6] Calvayrac F, Reinhard P-G, Suraud E and Ullrich C A 2000 *Phys. Rep.* **337** 493
[7] Tong X M and Chu S I 2001 *Phys. Rev.* A **64** 013417
[8] Castro A, Marques M A L, Alonso J A, Bertsch G F and Rubio A 2004 *Eur. Phys.* D **28** 211
[9] Livshits E and Baer R 2006 *J. Phys. Chem.* **110** 8443
[10] Yabana K and Bertsch G F 1999 *Int. J. Quantum Chem.* **75** 55
[11] Yabana K, Nakatsukasa T, Iwata J-I and Bertsch G F 2006 *Phys. Status Solidi* b **243** 1121
[12] Otobe T, Yamagiwa M, Iwata J-I, Yabana K, Nakatsukasa T and Bertsch G F 2008 *Phys. Rev.* B **77** 165104
[13] Castro A, Appel H, Oliveria M, Rozzi C A, Andrade X, Lorenzen F, Marques M A, Gross E K U and Rubio A 2006 *Phys. Status Solidi* b **243** 2465
[14] Kronik L, Makmal A, Tiago M L, Alemany M M G, Jain M, Huang X, Saad Y and Chelikowsky J R 2006 *Phys. Status Solidi* b **243** 1063
[15] Mundt M and Kümmel S 2007 *Phys. Rev.* B **76** 035413
[16] Yamanouchi K, Chin S L, Agostini P and Ferrante G (ed) 2006 *Progress in Ultrafast Intense Laser Science I-III* (*Springer Series in Chemical Physics* vol 84) (Berlin: Springer)
Yamanouchi K, Chin S L, Agostini P and Ferrante G (ed) 2007 *Progress in Ultrafast Intense Laser Science I-III* (*Springer Series in Chemical Physics* vol 85) (Berlin: Springer)
Yamanouchi K, Chin S L, Agostini P and Ferrante G (ed) 2008 *Progress in Ultrafast Intense Laser Science I-III* (*Springer Series in Chemical Physics* vol 89) (Berlin: Springer)
[17] Constant E, Stapelfeldt H and Neria J 1996 *Phys. Rev. Lett.* **79** 2022
[18] Frasinski L J, Codling K, Hatherly P, Barr J, Ross I N and Toner W T 1987 *Phys. Rev. Lett.* **58** 2424
[19] Otobe T, Yabana K and Iwata J-I 2004 *Phys. Rev.* A **69** 053404
[20] Frasinski L J, Codling K and Hatherly P A 1989 *Science* **246** 1029
[21] Hishikawa A, Iwamae A, Hoshina K, Kono M and Yamanouchi K 1998 *Chem. Phys. Lett.* **282** 283
[22] Ueyama M, Hasegawa H, Hishikawa A and Yamanouchi K 2005 *J. Chem. Phys.* **123** 154305
[23] Hishikawa A, Takahashi E J and Matsuda A 2006 *Phys. Rev. Lett.* **97** 243002
[24] Troullier N and Martins J L 1991 *Phys. Rev.* B **43** 1993
[25] Kleinman L and Bylander D 1982 *Phys. Rev. Lett.* **48** 1425
[26] Krieger J B, Li Y and Iafrate G J 1992 *Phys. Rev.* A **45** 101
[27] Chelikowsky J R, Troullier N, Wu K and Saad Y 1994 *Phys. Rev.* B **50** 11355
[28] Lappas D G and van Leeuwen R 1998 *J. Phys. B: At. Mol. Opt. Phys.* **31** L249
[29] Thiele M, Gross E K U and Kümmel S 2008 *Phys. Rev. Lett.* **100** 153004
[30] Mundt M and Kümmel S 2005 *Phys. Rev. Lett.* **95** 203004
[31] Isla M and Alonso J A 2005 *Phys. Rev.* A **72** 023201
[32] Andrae K, Dinh P M, Reinhard P-G and Suraud E 2006 *Comput. Mater. Sci.* **35** 169
[33] Laarmann T *et al* 2007 *Phys. Rev. Lett.* **98** 058302
[34] Körzdörfer T, Mundt M and Kümmel S 2008 *Phys. Rev. Lett.* **100** 133004
[35] Messud J, Dinh P M, Reinhard P-G and Suraud E 2008 *Phys. Rev. Lett.* **101** 096404